

Electronic supplementary information

of

Tungsten nitride-based degradable nanoplatform for dual-modal image-guided combinatorial chemo-photothermal therapy of tumors

Cheng Zhang^{†,#}, Shi-Bo Wang^{†,§,#}, Zhao-Xia Chen[†], Jin-Xuan Fan[†], Zhen-Lin Zhong^{†,*} and Xian-Zheng Zhang^{†,§,*}

[†]Key Laboratory of Biomedical Polymers of Ministry of Education and Department of Chemistry, Wuhan University, Wuhan 430072, P. R. China

[§]The Institute for Advanced Studies, Wuhan University, Wuhan 430072, P. R. China

*E-mails: zlzhong@whu.edu.cn, xz-zhang@whu.edu.cn

#These authors contributed equally to this work.

Table S1 Photothermal conversion efficiency of some representative PTAs.

PTAs	Photothermal Conversion Efficiency (%)	References
Au nanorods	21	<i>Nano Lett.</i> 2011, 11, 2560-2566
Graphene oxide	25	<i>Chem. Commun.</i> 2014,50, 14345-14348
Cu_9S_5	25.7	<i>Adv. Mater.</i> 2014, 26, 3433-3440
MoS_2 nanosheets	24	<i>ACS Nano.</i> 2014, 8, 6922-6933

Table S2 Hydrodynamic size and zeta potential of various samples in aqueous solution.

Samples	Size (PDI)	Zeta Potential (mV)
PEG-WN	143 ± 12 (0.21)	-0.33 ± 0.11
PEG-WN-DOX	156 ± 13 (0.18)	-0.51 ± 0.15

Table S3 Blood biochemistry data of the mice after 12 days of treatments.

Groups	ALB (g/L)	AST (U/L)	UREA (mM/L)	ALT (U/L)
PBS	30.6 ± 0.4	96.5 ± 17.5	8.3 ± 0.4	48.5 ± 2.5
DOX	27.4 ± 0.6	129.2 ± 24.2	5.2 ± 0.3	33.0 ± 3.5
PEG-WN	30.6 ± 0.5	99.3 ± 14.7	7.2 ± 0.3	49.0 ± 5.3
PEG-WN + Laser	31.3 ± 0.4	94.6 ± 12.5	8.2 ± 0.4	47.5 ± 4.3
PEG-WN-DOX	28.9 ± 0.4	93.5 ± 19.0	8.4 ± 0.2	45.0 ± 5.6
PEG-WN-DOX + Laser	30.6 ± 0.7	101.7 ± 15.8	7.9 ± 0.3	51.4 ± 4.6

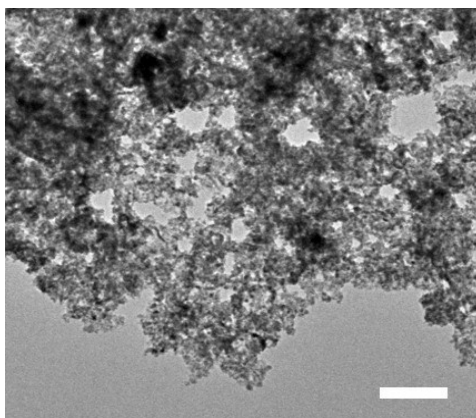


Fig. S1 TEM image of the as-prepared bulk WN. Scale bar: 200 nm.

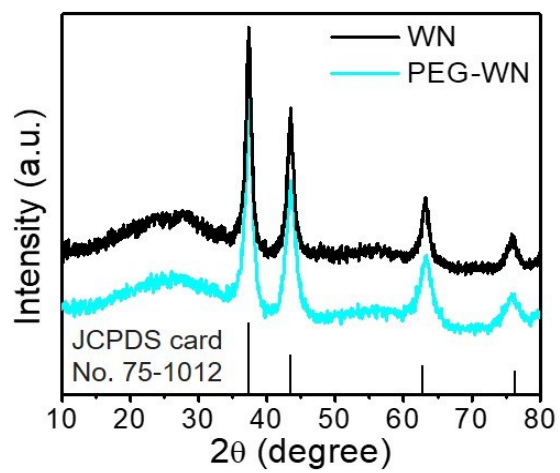


Fig. S2 XRD pattern of WN and the as-prepared PEG-WN NPs.

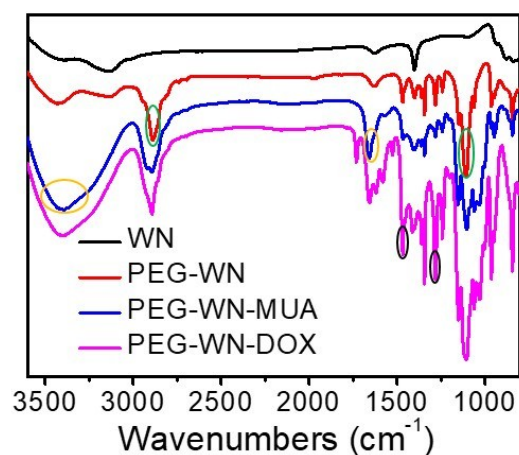


Fig. S3 Infrared spectra of WN, PEG-WN, PEG-WN-CD, and PEG-WN-DOX. The green circles show the new peaks of C-O and -CH₂ at 1108 cm⁻¹ and 2889 cm⁻¹, respectively, which confirm the successful bonding of PEG on the surface of WN. The yellow circles show the strengthened peaks of -OH at 3395 cm⁻¹ and 1658 cm⁻¹, which arose from (2-Hydroxypropyl)- β -cyclodextrin. The black circles show the new peaks at 1470 cm⁻¹ and 1284 cm⁻¹, which are due to the carbon vibration of benzene ring in DOX.

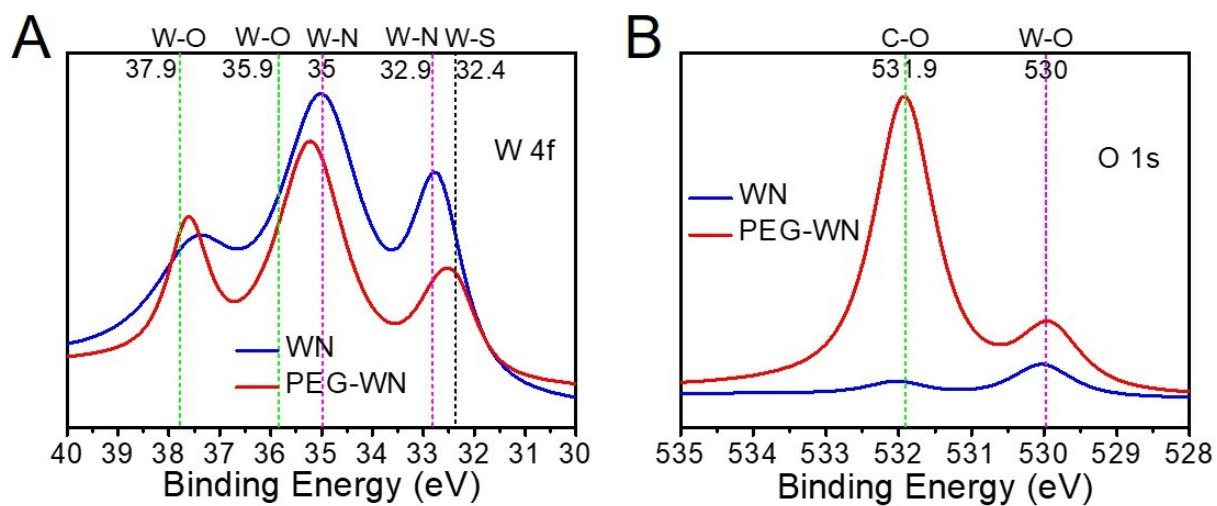


Fig. S4 XPS spectra for (A) W 4f and (B) O 1s of WN and PEG-WN. The shift of the W 4f peak to right at 32.4 eV and the appearance of strong O 1s peak at 531.9 eV indicated the successful coating of SH-PEG on the surface of WN NPs through the formation of W-S bond.^{S1}

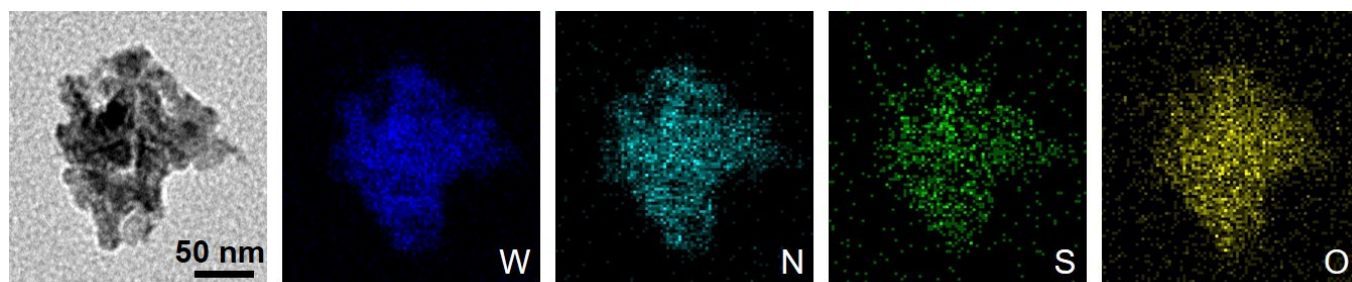


Fig. S5 TEM image and corresponding element mapping of PEG-WN.

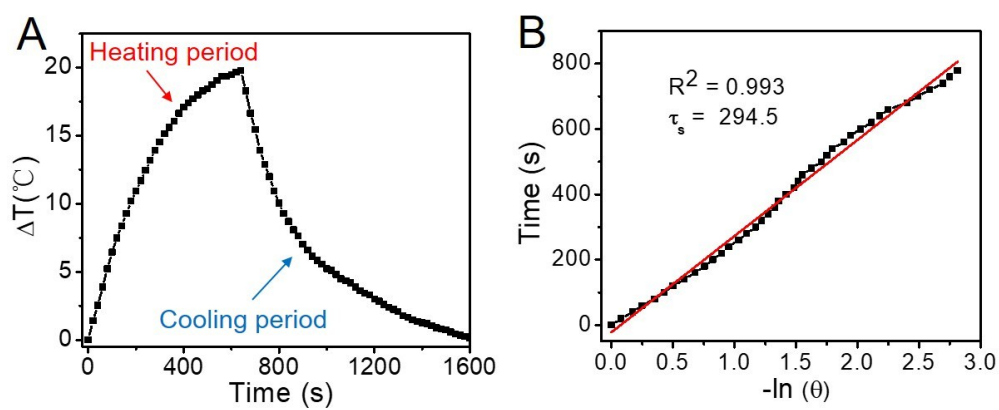


Fig. S6 Heating/cooling experiment of PEG-WN NPs (40 $\mu\text{g}/\text{mL}$) under the 808 nm laser irradiation.

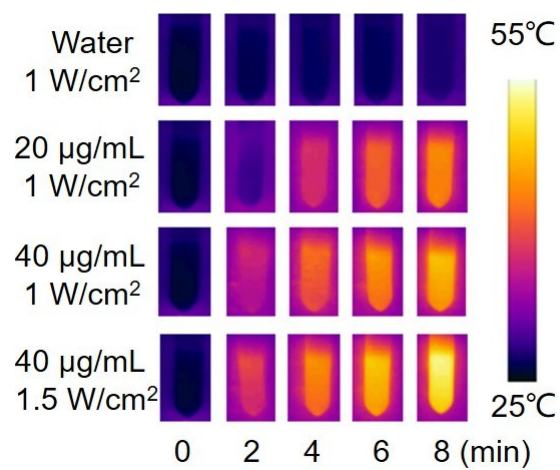


Fig. S7 Thermal images of PEG-WN NPs with different concentrations recorded by an IR camera during 808 nm laser irradiation.

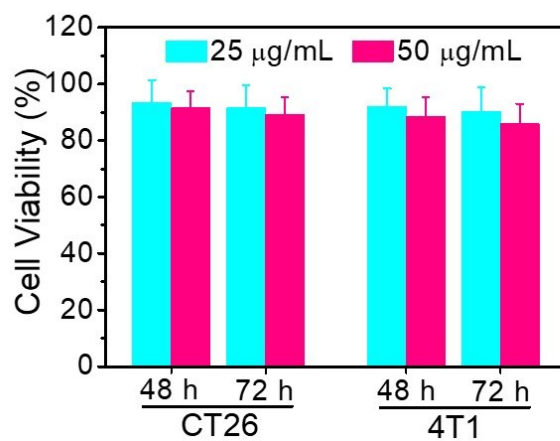


Fig. S8 Cell viability of CT26 and 4T1 cells after co-incubation with PEG-WN NPs with 25 and 50 µg/mL for 48 and 72 h.

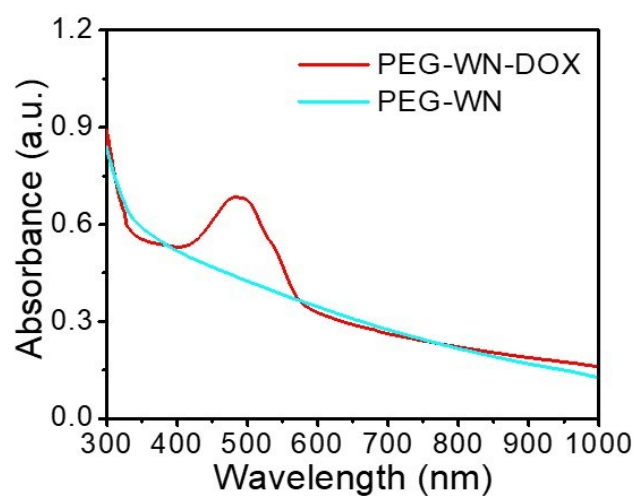


Fig. S9 UV/Vis-NIR absorbance spectra of PEG-WN-DOX and PEG-WN NPs in water.

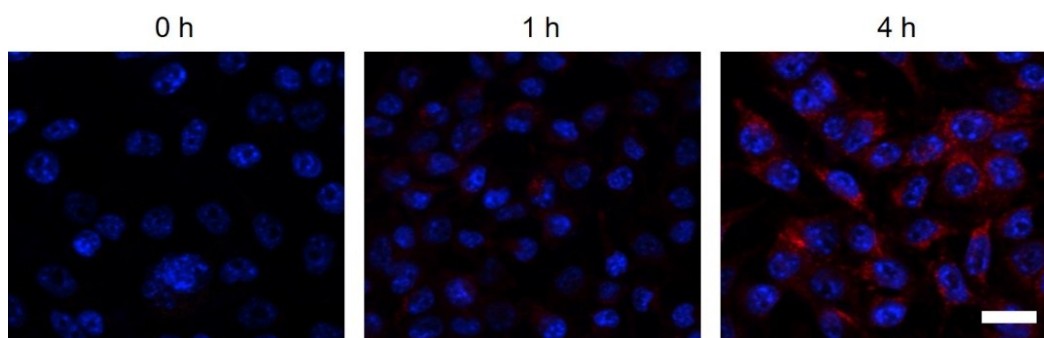


Fig. S10 Intracellular delivery of PEG-WN-DOX towards CT26 cells at different time points observed by confocal laser scanning microscopy. (The nuclei were stained with Hoechst 33342. Scale bar: 20 μm .)

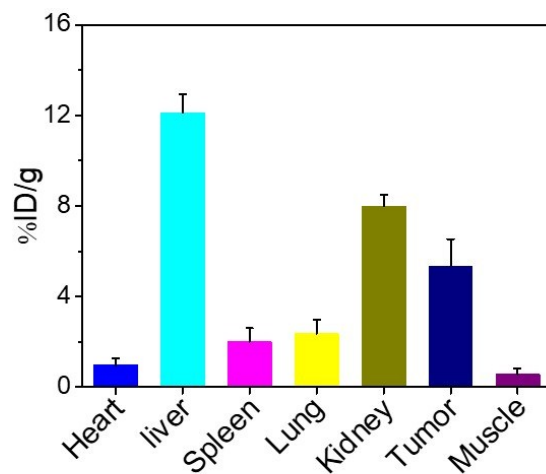


Fig. S11 Tungsten level in major organs 24 h post i.v. injection of PEG-WN NPs.

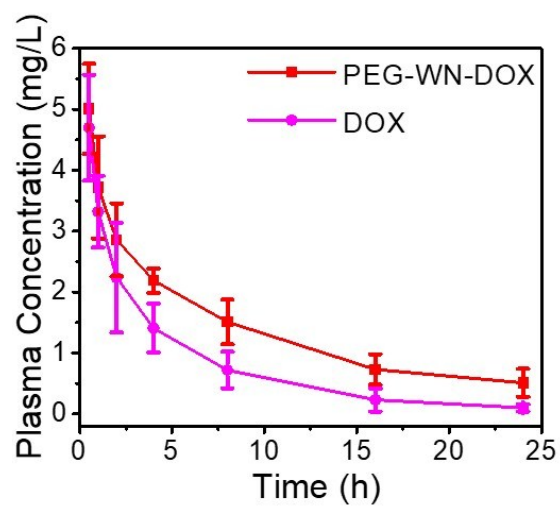


Fig. S12 Pharmacokinetics of DOX after i.v. injection of the free DOX and PEG-WN-DOX NPs into mice at DOX dose of 0.6 mg/kg.

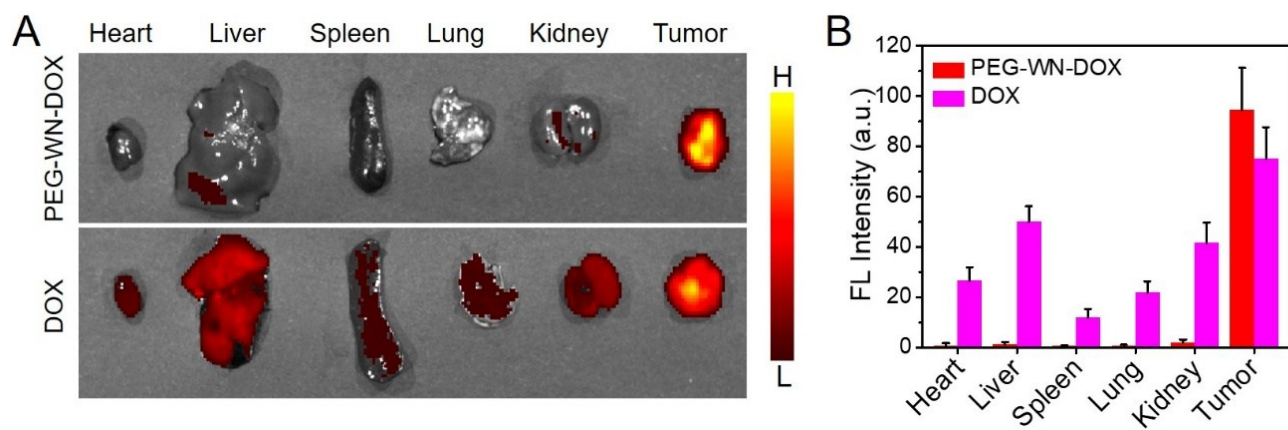


Fig. S13 (A) Fluorescence images and (B) the corresponding fluorescence intensity of free DOX and PEG-WN-DOX NPs 24 h post injection in tumors and major organs.

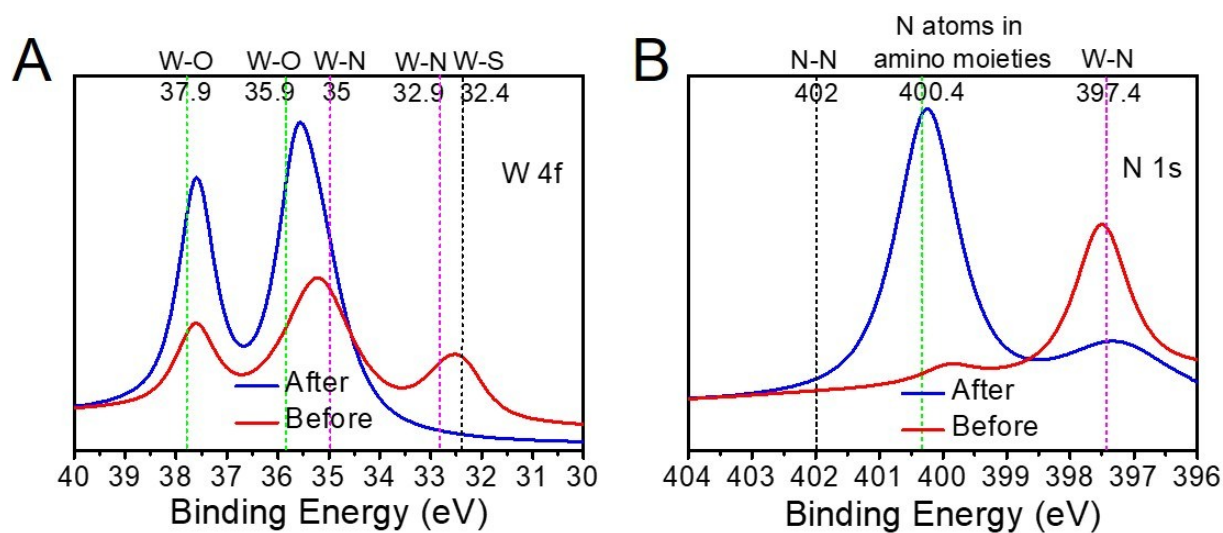


Fig. S14 XPS spectra for (A) W 4f and (B) N 1s of PEG-WN before and after oxidative degradation for 30 days in water. The enhancement of W 4f peaks at 35.9 eV and 37.9 eV and N 1s peak at 400.4 eV indicated the formation of ammonium metatungstate hydrate.^{S2}

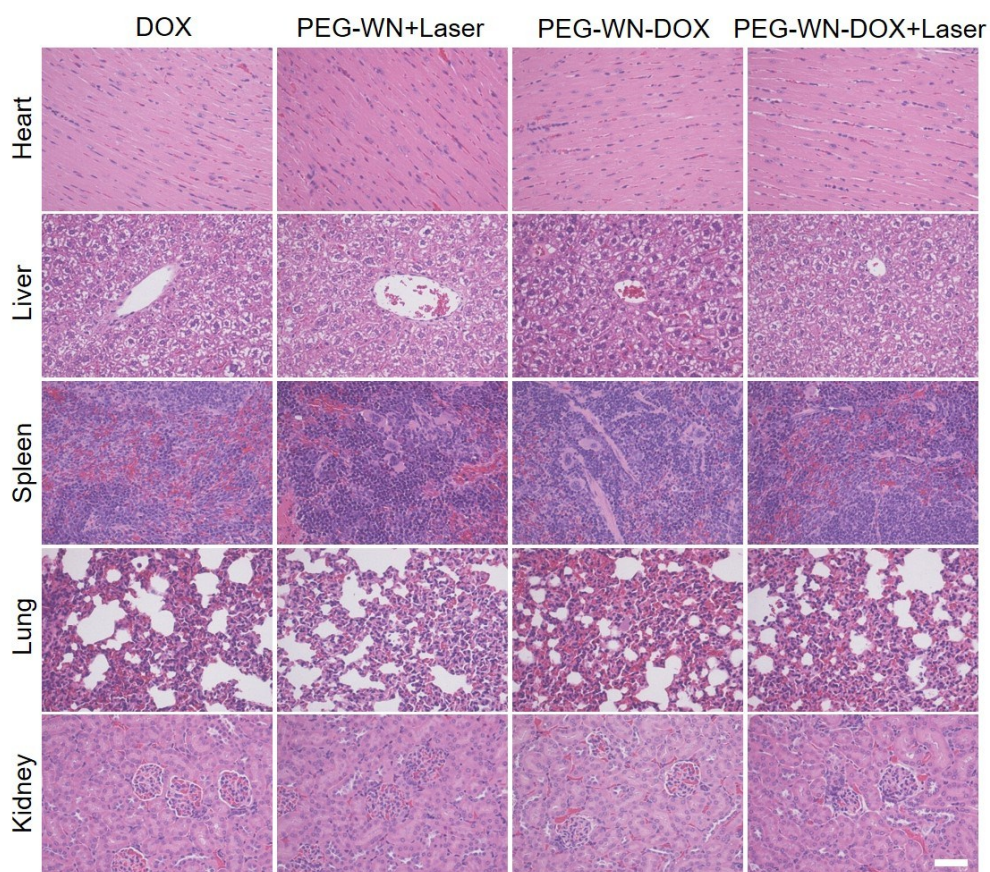


Fig. S15 H&E staining of major organs from different groups after 12-day treatment.

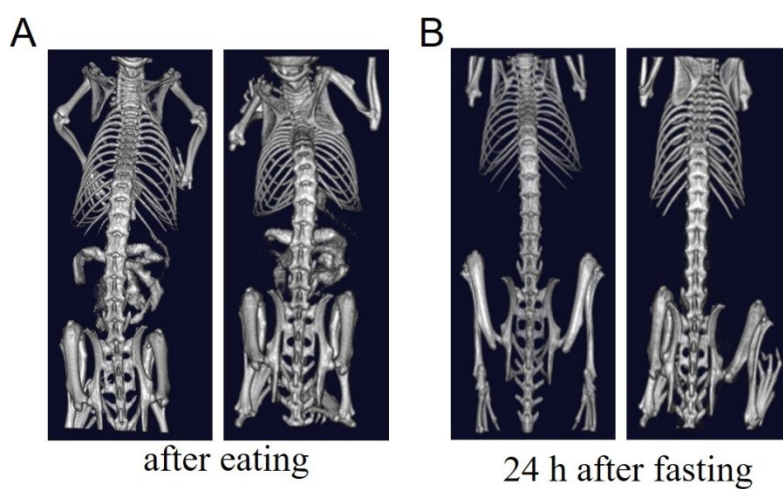


Fig. S16 Whole body CT scans of mice (A) after eating and (B) 24 h after fasting.

References

- S1. J. Ren, Z. Wang, F. Yang, R. P. Ren, Y. K. Lv, *Electrochim. Acta* 2018, **267**, 133-140.
- S2. F. Chang, J. Zheng, F. Wu, X. Wang, B. Deng, *Colloids and Surfaces A: Physicochem. Eng. Aspects* 2019, **563**, 11-21.